11-2019

# InAs(111)A Homoepitaxy with Molecular Beam Epitaxy

Kevin D. Vallejo
*Boise State University*

Trent A. Garrett
*Boise State University*

Kathryn E. Sautter
*Boise State University*

Kevin Saythavy
*Boise State University*

Baolai Liang
*University of California Los Angeles*

*See next page for additional authors*

# InAs(111)A homoepitaxy with molecular beam epitaxy

Kevin D. Vallejo,[1] Trent A. Garrett,[2] Kathryn E. Sautter,[1] Kevin Saythavy,[1] Baolai Liang,[3] and Paul J. Simmonds[1,2,a)]
[1]*Micron School of Materials Science & Engineering, Boise State University, Boise, Idaho 83725*
[2]*Department of Physics, Boise State University, Boise, Idaho 83725*
[3]*California NanoSystems Institute, University of California Los Angeles, Los Angeles, California 90095*

(Received 13 September 2019; accepted 28 October 2019; published 14 November 2019)

The authors have established a robust set of growth conditions for homoepitaxy of high-quality InAs with a (111)A crystallographic orientation by molecular beam epitaxy (MBE). By tuning the substrate temperature, the authors obtain a transition from a 2D island growth mode to step-flow growth. Optimized MBE parameters (substrate temperature = 500 °C, growth rate = 0.12 ML/s, and V/III ratio ≥ 40) lead to the growth of extremely smooth InAs(111)A films, free from hillocks and other 3D surface imperfections. The authors see a correlation between InAs surface smoothness and optical quality, as measured by photoluminescence spectroscopy. This work establishes InAs(111)A as a platform for future research into other materials from the 6.1 Å family of semiconductors grown with a (111) orientation. *Published by the AVS.* https://doi.org/10.1116/1.5127857

## I. INTRODUCTION

In recent years, there has been renewed interest in epitaxial growth on the (111) surfaces of III-V semiconductors. This resurgence is driven by the unique properties of this crystallographic orientation, which are attractive for a range of emerging technologies.[1] A high quality, (111)-oriented material is needed for transistors where electron transport occurs in both Γ and *L* valleys;[2] quantum dots with negligible fine-structure splitting for entangled photon sources;[3,4] $V_2$–$VI_3$ topological insulators whose crystalline quality benefits from the threefold symmetry of the (111) surface;[5,6] and transition metal dichalcogenides and other 2D materials since the (111) surfaces lend themselves well to van der Waals epitaxy.[7,8]

Before we can unlock the full potential of (111) surfaces, we must first overcome the challenge of growing semiconductors with this orientation, since the growth on (111) is frequently more difficult than the growth on traditional (001) substrates. The formation of large 3D hillocks during molecular beam epitaxy (MBE) can impair the optical and electronic properties of these materials.[1] As a result of considerable research efforts, high-quality, (111)-oriented materials can now be grown on some of the most commonly used III-V substrates. Growth conditions have been optimized for the A and B faces of GaAs(111).[9–16] Similarly, several papers explore the MBE parameters for homoepitaxy of InP(111), as well as for heteroepitaxy of its technologically relevant lattice-matched alloys, $In_{0.52}Al_{0.48}As$ and $In_{0.53}Ga_{0.47}As$.[4,17–19]

In contrast, few studies exist concerning the growth of InAs(111)A.[20–23] Reference 20 demonstrates rough InAs(111)A surfaces covered in a high density of hillocks, while Refs. 22 and 24 grew only very thin films (<30 nm) for low-temperature scanning tunneling microscopy, which would not be thick enough for future device structures.[22,24] A systematic study of the effects of MBE growth conditions on InAs(111)A morphology and material quality has not yet been reported.

Establishing the MBE growth of InAs(111)A would open up research areas requiring (111)-oriented growth with lower bandgaps than can be reached with the GaAs and InP materials systems. In addition, the growth of high-quality InAs(111)A would provide access to other (111)-oriented semiconductors in the 6.1 Å materials family.[25] With a lattice constant of 6.058 Å, InAs is almost lattice matched to GaSb and AlSb (6.096 Å and 6.136 Å, respectively), as well as to several II-VI semiconductors. Monolithic integration of these 6.1 Å materials on (111) surfaces would create the opportunity for developing heterostructures with previously unavailable functionalities.[25]

In this paper, we add InAs(111)A to the list of III-V substrates for which homoepitaxial growth conditions have been comprehensively studied. We determine the MBE growth conditions required for minimizing surface roughness and maximizing material quality. We show that the growth of InAs(111)A is particularly sensitive to the careful choice of the substrate temperature.

## II. METHODS

Using an indium effusion cell and a valved $As_4$ source, we use MBE to grow InAs on pieces of unintentionally doped InAs(111)A substrate. We use $As_4$ for consistency with existing literature reports, most of which use this As species.[20,23] Since (111)A substrates cleave preferentially along the $[\bar{1}10]$, $[10\bar{1}]$, and $[0\bar{1}1]$ directions, the resulting pieces are triangles and parallelograms, which are incompatible with indium-free sample holders. We, therefore, use high-purity indium metal to mount the cleaved InAs(111)A pieces onto molybdenum blocks, an approach that provides excellent temperature uniformity across the sample. We monitor substrate temperature, $T_{sub}$, using a thermocouple behind the substrate and an infrared pyrometer, calibrated against known changes in surface reconstruction using reflection high-energy electron diffraction (RHEED). We remove the InAs

a)Electronic mail: paulsimmonds@boisestate.edu

surface oxide by heating the substrate under $As_4$ to $T_{sub} = 495\,^{\circ}C$, annealing it for 600 s, and then annealing at 500 °C for a further 180 s. We then adjust $T_{sub}$ to the required growth temperature. After oxide desorption, RHEED shows a clear $(2 \times 2)$ surface reconstruction. Using RHEED intensity oscillations performed on the (001) surface, we calculate growth rates (GRs) on (111)A in monolayers per second (ML/s).

To identify optimal MBE conditions for InAs(111)A homoepitaxy, we grew three experimental series, each sample consisting of 100 nm InAs, to explore the effects of changing (i) $T_{sub}$ from $380 - 520\,^{\circ}C$; (ii) InAs growth rate from 0.06–0.24 ML/s; and (iii) and $As_4$/In V/III atomic flux ratio from 12 to 48. For a given In flux in atoms $cm^{-2}\,s^{-1}$, we find the equivalent atomic As flux by reducing the As until we see a transition from the As-stabilized $(2 \times 4)$ reconstruction to the In-stabilized $(4 \times 2)$ reconstruction on InAs(001). We use multiples of the corresponding As beam equivalent pressure to obtain any desired V/III atomic flux ratio. After growth, we anneal samples under $As_4$ at the growth temperature for 180 s to promote surface smoothing,[23] before cooling under $As_4$. We characterize InAs surface morphology using atomic force microscopy (AFM), and calculate the root mean square roughness, $R_q$, from $1 \times 1\,\mu m^2$ AFM images (unless otherwise noted). We characterize the material quality using room-temperature photoluminescence (PL) spectroscopy. We also explored the use of x-ray diffraction and Raman spectroscopy to measure crystal quality. However, these techniques did not provide sufficient resolution to distinguish between the best and worst of the samples in this study, and so the results are not discussed here. All error bars in this study show the standard deviation across multiple measurements, divided by the square root of the number of measurements.

## III. RESULTS

### A. Substrate temperature variation

InAs(111)A material quality is strongly dependent on $T_{sub}$, with both surface morphology and PL intensity optimized in the range $470 - 500\,^{\circ}C$.

We grew a series of InAs(111)A samples at $T_{sub} = 380$, 410, 440, 470, 500, and 520 °C, while holding the growth rate and V/III ratio constant at 0.12 ML/s and 24, respectively. At $T_{sub} \leq 440\,^{\circ}C$, growth proceeds by the formation of 2D flat, monolayer-high islands that show no preferential growth direction [Figs. 1(a)–1(c)]. Between $T_{sub} = 470$ and 500 °C, we see a transition from layer-by-layer growth to step-flow growth, with the formation of long terraces [Figs. 1(d) and 1(e)]. As well as this change in growth mode, raising $T_{sub}$ from 380 °C to 500 °C also smooths the InAs(111)A surface, lowering $R_q$ from 4.9 to 1.4 Å. However, increasing $T_{sub}$ further, to 520 °C, has the opposite effect, roughening the InAs(111)A surface, predominantly as a result of step-bunching [Fig. 1(f)].

Samples grown at $T_{sub} \geq 440\,^{\circ}C$ exhibit a twofold increase in PL intensity, compared to samples grown at lower temperature [Fig. 1(g)]. Defects such as dislocations and mid-gap trap states can act as nonradiative recombination centers, reducing PL intensity. The brighter PL we see for $T_{sub} \geq 440\,^{\circ}C$, therefore, suggests that the material quality is enhanced in samples grown at a higher temperature.

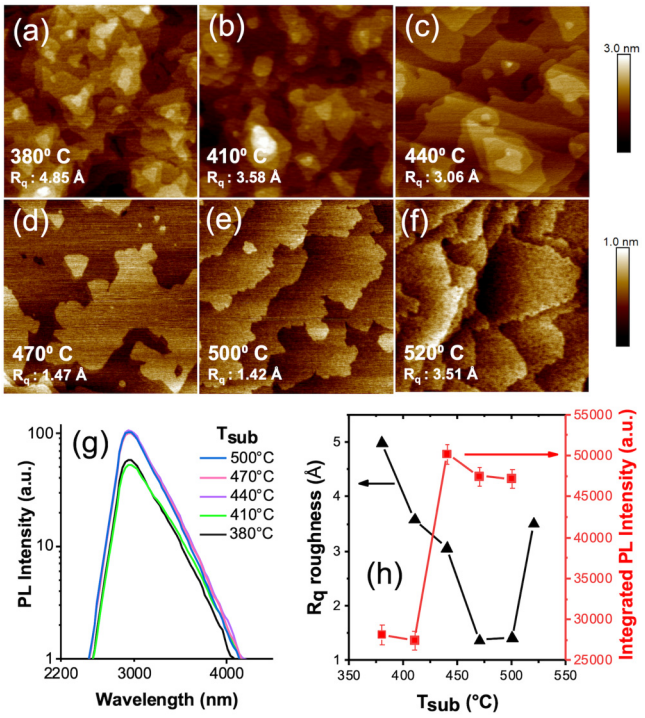


FIG. 1. (a)–(f) $1 \times 1\,\mu m^2$ AFM micrographs showing the effect of $T_{sub}$ on InAs(111)A surface morphology. The height for (a)–(c) is 3 nm while for (d)–(f) it is 1 nm. All samples were grown at 0.12 ML/s, with a V/III ratio of 24. A dramatic decrease in $R_q$ surface roughness above $T_{sub} = 440\,^{\circ}C$ is accompanied by a transition from island growth to step-flow growth. (g) InAs(111)A PL spectra as a function of $T_{sub}$. PL is brighter for samples grown at a higher temperature, consistent with improved material quality. (h) Triangles show $R_q$ (over a $1\,\mu m^2$ area) as a function of $T_{sub}$, with roughness minimized at $470 - 500\,^{\circ}C$. Squares show the integrated intensity of the PL spectrum for each $T_{sub}$ sample. We see a sharp increase in light emission intensity above $T_{sub} = 410\,^{\circ}C$.

Figure 1(h) illustrates that we can obtain extremely smooth InAs(111)A and bright PL emission simultaneously. From these results, one should grow InAs(111)A at $T_{sub} = 470 - 500\,^{\circ}C$ for optimal material quality.

### B. Growth rate variation

InAs(111)A material quality is weakly dependent on InAs GR, with both surface smoothness and PL intensity optimized in the range 0.06–0.12 ML/s.

We grew a series of InAs(111)A samples with growth rates of 0.06, 0.12, and 0.24 ML/s, while holding $T_{sub}$ at 500 °C, based on the results above. For each sample, we adjusted the $As_4$ flux to maintain a constant V/III ratio of ~24.

All three samples exhibit a step-flow morphology. Looking at $5 \times 5\,\mu m^2$ areas of the samples, $R_q$ roughness decreases monotonically with increasing growth rate [Figs. 2(a)–2(c)]. However, at higher magnification (insets of Fig. 2), the sample grown at 0.12 ML/s shows the smoothest surface due to its long terraces, $\sim 1\,\mu m$ wide.

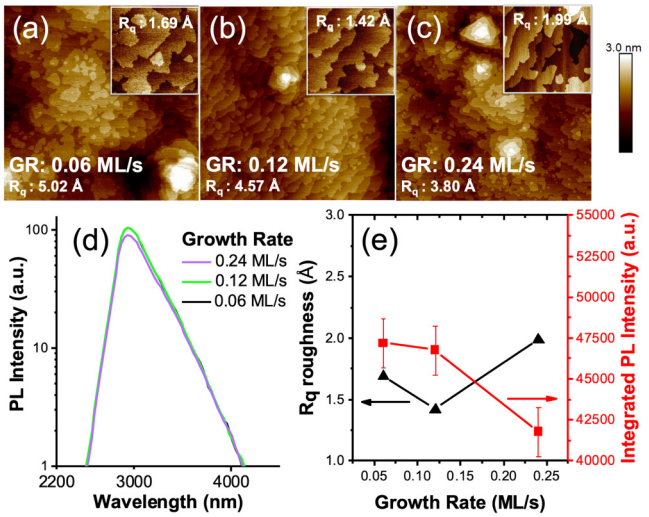


FIG. 2. (a)–(c) AFM micrographs showing the effect of InAs(111)A growth rate on surface morphology. All samples were grown at 500 °C, with a V/III ratio of 24. Large figures are $5 \times 5\,\mu m^2$ scans with a height of 3 nm, with insets of $1 \times 1\,\mu m^2$ and a height of 1 nm. (d) InAs(111)A PL spectra as a function of the sample growth rate. These spectra are similar in intensity, indicating that InAs(111)A optical quality is only weakly dependent on the growth rate. (b) Triangles show $R_q$ (over a $1\,\mu m^2$ area) as a function of the InAs(111)A growth rate, with the lowest roughness occurring at 0.12 ML/s. Squares show the integrated intensity of the PL spectrum for each growth rate. PL intensity decreases at the highest growth rate, and the surface becomes rougher.

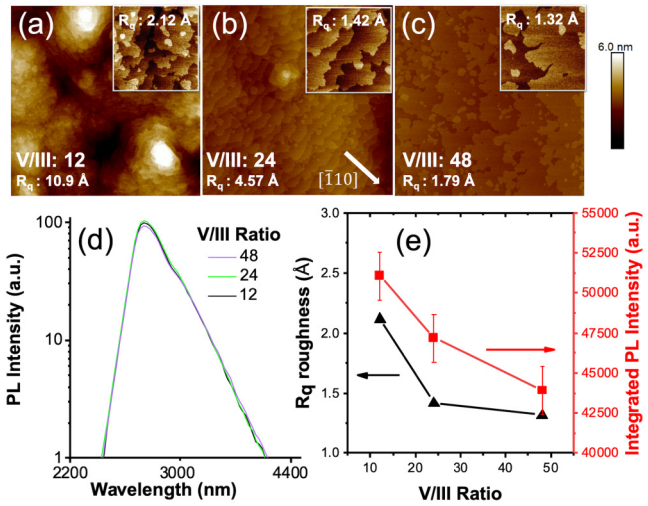


FIG. 3. $5 \times 5\,\mu m^2$ AFM micrographs showing the effect of V/III ratio on surface morphology. All samples were grown at 500 °C, with a growth rate of 0.12 ML/s. Large images have a height of 6 nm, with insets of $1 \times 1\,\mu m^2$ and a height of 1 nm. For V/III > 12, we see smooth InAs(111)A surfaces and the formation of regularly spaced terraces aligned perpendicular to the [$\bar{1}$10] direction. (d) InAs(111)A PL spectra as a function of V/III ratio. The spectra are reasonably close in intensity, indicating limited dependence of V/III ratio on InAs(111)A optical quality. (e) Triangles show $R_q$ (over a $1\,\mu m^2$ area) as a function of V/III ratio, showing that ratios above 24 result in the smoothest film growth. Squares show the integrated intensity of the PL spectrum for each V/III ratio sample. Although there is a small downward trend with the increased V/III ratio, the magnitude of the change is almost within the measurement error.

The 0.06 ML/s and 0.12 ML/s samples show almost identical PL emission, with a slight decrease in intensity for the sample grown at 0.24 ML/s [Fig. 2(d)]. The small reduction in PL intensity suggests that at higher growth rate, shorter adatom migration lengths may introduce point defects so that material quality starts to suffer.

Figure 2(e) shows that by growing more slowly, we can optimize InAs(111)A surface smoothness and optical quality at the same time. Given that the surface morphology of the sample grown at 0.12 ML/s presents the lowest roughness and bright optical emission, we recommend using this growth rate.

### C. V/III ratio variation

InAs(111)A material quality is weakly dependent on V/III flux ratio, with surface smoothness and PL intensity optimized in the range 24–48.

We grew a series of InAs(111)A samples with V/III flux ratios of 12, 24, and 48, while holding $T_{sub}$ and growth rate constant at 500 °C and 0.12 ML/s, respectively, based on the results above.

At a V/III ratio of 12, we observe the growth of "wedding cakes" (concentric stacks of 2D islands), ~7 nm tall, across the sample surface. Increasing the V/III ratio to 24 produces a significantly smoother surface, where a step-flow growth can be seen around the wedding cakes. For V/III ratios ~48, InAs(111)A growth transitions fully into a step-flow mode with atomically flat terraces, ~1 $\mu$m wide [Figs. 3(a)–3(c)].

PL intensity declines slightly with increasing V/III ratio, over the range studied here, which could indicate a reduction in material quality, possibly due to the formation of As antisite defects. Alternatively, it is possible that as the InAs becomes extremely smooth [Fig. 3(c)], outcoupling of photons from the sample is reduced, lowering the measured PL intensity.[26] The PL intensities of the three samples measured are within 1.5 standard deviations of each other [Fig. 3(e)]. To put this in context, the standard deviation of the intensity from these three samples intensities is comparable to the difference in intensity we see between PL measurements done at different locations on the same sample.

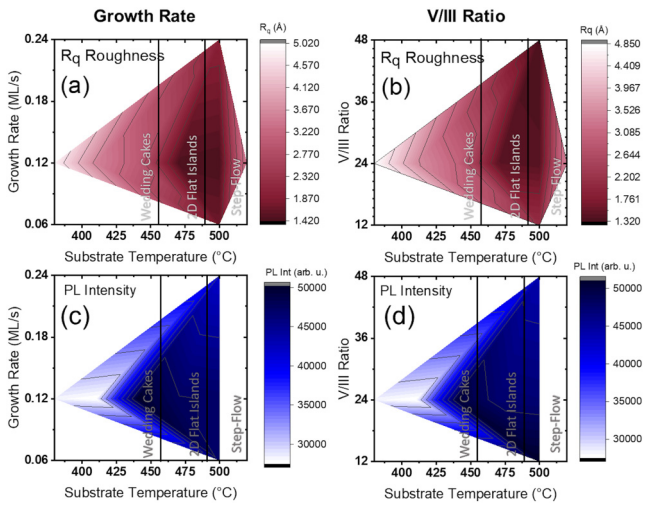


FIG. 4. Contour plots of $R_q$ roughness as a function of (a) growth rate and $T_{sub}$, (b) V/III ratio and $T_{sub}$. Contour plots of integrated PL intensity as a function of (c) growth rate and $T_{sub}$, and (d) V/III ratio and $T_{sub}$. Darker regions indicate improved material parameters: (a) and (b) have darker tones (magenta in color) for smoother surfaces, while in (c) and (d) darker tones (blue in color) indicate higher integrated PL intensity.

Plotting InAs(111)A $R_q$ and integrated PL intensity as a function of V/III ratio [Fig. 3(e)], the situation differs from what we saw for $T_{sub}$ [Fig. 1(h)] and InAs growth rate [Fig. 2(e)]. For the V/III ratio series, there does not seem to be an analogous correlation between smoother surfaces and enhanced material quality. However, since the optical quality seems to remain fairly high regardless of the V/III ratio used, it makes sense to optimize V/III ratio in order to achieve the smoothest InAs(111)A, and so we recommend V/III flux ratios of ~48.

### D. Summary of growth conditions

Figure 4 summarizes the MBE conditions that lead to smooth, high-quality homoepitaxial InAs(111)A. Figures 4(a)–4(b) show how surface roughness is minimized at $T_{sub} = 475 - 500\,^{\circ}C$ when we use a growth rate of 0.12 ML/s and V/III ratios of 24–48. Figures 4(c) and 4(d) show that PL intensity is also brightest when these growth conditions are used, confirming that we can simultaneously optimize both InAs(111)A surface morphology and optical quality.

## IV. CONCLUSIONS

We have established a set of MBE growth parameters that yields exceptionally smooth InAs(111)A homoepitaxial films with atomically flat terraces, $>1\,\mu$m in width, and optimal optical quality. The ability to grow smooth, high-quality InAs(111)A films opens up opportunities for research into other 6.1 Å semiconductors that share this technologically relevant surface orientation.

## ACKNOWLEDGMENT

The authors acknowledge financial support from the College of Engineering, Boise State University.

[1]C. D. Yerino, B. Liang, D. L. Huffaker, P. J. Simmonds, and M. L. Lee, J. Vac. Sci. Technol. B **35**, 010801 (2017).
[2]S. R. Mehrotra, M. Povolotskyi, D. C. Elias, T. Kubis, J. J. Law, M. J. Rodwell, and G. Klimeck, IEEE Electron Device Lett. **34**, 1196 (2013).
[3]A. Schliwa, M. Winkelnkemper, A. Lochmann, E. Stock, and D. Bimberg, Phys. Rev. B **80**, 161307(R) (2009).
[4]C. D. Yerino *et al.*, Appl. Phys. Lett. **105**, 251901 (2014).
[5]N. V. Tarakina, S. Schreyeck, T. Borzenko, C. Schumacher, G. Karczewski, K. Brunner, C. Gould, H. Buhmann, and L. W. Molenkamp, Cryst. Growth Des. **12**, 1913 (2012).
[6]Z. Zeng *et al.*, AIP Adv. **3**, 072112 (2013).
[7]K. Ueno, T. Shimada, K. Saiki, and A. Koma, Appl. Phys. Lett. **56**, 327 (1990).
[8]S. Vishwanath *et al.*, J. Mater. Res. **31**, 900 (2016).
[9]Y. Okano, M. Shigeta, H. Seto, H. Katahama, S. Nishine, and I. Fujimoto, Jpn. J. Appl. Phys. **29**, L1357 (1990).
[10]D. Woolf, D. Westwood, and R. Williams, Semicond. Sci. Technol. **8**, 1075 (1993).
[11]M. R. Fahy, K. Sato, and B. A. Joyce, Appl. Phys. Lett. **64**, 190 (1994).
[12]K. Sato, M. R. Fahy, and B. A. Joyce, Jpn. J. Appl. Phys. **33**, L905 (1994).
[13]P. Chen, K. C. Rajkumar, and A. Madhukar, Appl. Phys. Lett. **58**, 1771 (1991).
[14]C. Guerret-Piecourt and C. Fontaine, J. Vac. Sci. Technol. B **16**, 204 (1998).
[15]P. J. Simmonds and M. L. Lee, Appl. Phys. Lett. **99**, 10 (2011).
[16]P. J. Simmonds and M. L. Lee, J. Appl. Phys. **112**, 054313 (2012).
[17]H. Q. Hou and C. W. Tu, Appl. Phys. Lett. **62**, 281 (1993).
[18]I. Sadeghi, M. C. Tam, and Z. R. Wasilewski, J. Vac. Sci. Technol. B **37**, 031210 (2019).
[19]C. F. Schuck, R. A. McCown, A. Hush, A. Mello, S. Roy, J. W. Spinuzzi, B. Liang, D. L. Huffaker, and P. J. Simmonds, J. Vac. Sci. Technol. B **36**, 031803 (2018).
[20]K. Sugiyama, J. Cryst. Growth **75**, 435 (1986).
[21]J. A. Dura, J. T. Zborowski, and T. D. Golding, Mater. Res. Soc. Symp. Proc. **263**, 35 (1992).
[22]J. Yang, C. Nacci, J. Martínez-Blanco, K. Kanisawa, and S. Fölsch, J. Phys. Condens. Matter **24**, 354008 (2012).
[23]K. Kanisawa, J. Cryst. Growth **378**, 8 (2013).
[24]A. Taguchi and K. Kanisawa, Appl. Surf. Sci. **252**, 5263 (2006).
[25]H. Kroemer, Physica E **20**, 196 (2004).
[26]K. Neyts, Appl. Surf. Sci. **244**, 517 (2005).